Raman spectrum of hcp solid ^{4}He

Norio Ogita, Masayuki Udagawa, and Kohji Ohbayashi
Faculty of Integrated Arts and Sciences, Hiroshima University, Hiroshima 730, Japan
(Received 1 December 1992)

Raman spectra of hcp solid ^{4}He have been measured at a temperature of 0.71 K with an instrumental resolution of 1.1 cm^{-1}. The spectra have been confirmed to be consistent with those reported by former works: a sharp one-phonon peak is observed at 7.39±0.06 cm^{-1}, the two-phonon spectrum appears in the energy region about 10–45 cm^{-1}, and a broad continuous tail extends to energy shifts higher than the two-phonon region. Four peaks have been resolved in two-phonon spectra at 17.1, 20.9, 25.2, and about 30 cm^{-1}. The two-phonon spectral structure has good qualitative similarity to that calculated theoretically by former workers. This verifies that the two-phonon spectral structure can be used for quantitative determination of parameters of lattice dynamics in quantum solids, and necessary experimental accuracy and resolution are discussed.

I. INTRODUCTION

Raman scattering from liquids and solids is a powerful and often unique probe of their elementary excitations. In fact, recently, fine structures have been confirmed for superfluid ^{4}He, which are useful to investigate interactions between elementary excitations.[1–3] For hcp helium solids, a strong and sharp one-phonon peak at the Brillouin-zone center and two-phonon peaks, mainly due to zone-boundary phonons, are expected. Observation of those peaks gives us information on the dispersion relations of phonons and sometimes possibly interactions between them. Raman scattering is a less direct method to investigate phonon-dispersion relations compared with neutron scattering in that the momentum condition is restricted. However, the latter method is extremely difficult to apply to helium solids, which include ^{3}He isotopes due to absorption of neutrons by ^{3}He atoms. Therefore Raman scattering is not only complementary to neutron scattering but also expected to be unique in the study of helium solids which include ^{3}He isotopes.

Historically, research on the phonon dispersion relations in solid helium was done mostly nearly 30 years ago. The phonon-dispersion relations in hcp ^{4}He solid were first studied experimentally with neutron inelastic scattering by Lipshultz *et al.*[4] in the symmetry direction of [10$\bar{1}$0] for wave vectors and Minkiewicz *et al.*[5] in the symmetry directions of [10$\bar{1}$0] and [0001]. Theoretical works were developed at the same time by Koehler[6,7] and Gillis and co-workers.[8,9] The neutron experimental results were found consistent with the theoretical calculations.[5,8] While those works on helium solids were carried out, Greytak and Yan[10] observed the two-roton Raman spectrum from superfluid ^{4}He by laser light-scattering experiment. Subsequently, Werthamer and co-workers calculated theoretical Raman spectra of helium solids, which postulated spectral structures by two-phonon processes as well as a sharp peak due to the first-order Raman scattering by a zone center optical-phonon model.[11,12]

Raman-scattering experiments on helium solids were carried out by Slusher and Surko.[13–15] They found the one-phonon Raman spectral peak at energy shifts consistent with the neutron results.[5] They also found a broad peak in the energy shift region where two-phonon Raman spectra were postulated. The work was an observation of those Raman processes. An anticipated observation was that they observed substantial continuous spectrum extending to the energy shift region far larger than that where two-phonon processes are expected. They attributed it to excitations of a pair of nearly free particles.

Recently we have carried out Raman scattering from hcp solid ^{4}He. The motivation to reinvestigate the spectrum observed almost 20 years ago was that we have recently confirmed a few fine structures in the Raman spectrum of superfluid ^{4}He.[1–3] The success of the observation for the superfluid ^{4}He lead us to extend to helium solids. Compared with those realized by the previous workers,[13–15] we improved the experimental conditions by decreasing the sample temperature and increasing the resolution of the spectrometer. Our observation on hcp solid ^{4}He clearly showed fine structure that may be assigned as two-phonon Raman-scattering processes, which were observed only as an unresolved broad single peak in the previous work.[15] Once detailed assignments of the two-phonon structures are established for solid ^{4}He, for which extended experimental theoretical studies were carried out, the resolved structures will be useful for study of helium solids including ^{3}He isotopes. To undertake those neutron studies will be very difficult.

II. EXPERIMENTAL APPARATUS

The optical arrangement of the experimental system is shown in Fig. 1. The incident light source was an argon-ion laser (Nippon Electric Company model No. GLG3200) operated at 514.5 nm with output power of 400 mW. Polarization of the beam from the source was vertical. To determine the direction of polarization of the beam incident on the sample arbitrarily, the polarization rotator and the polarizer 1 were used. The beam was

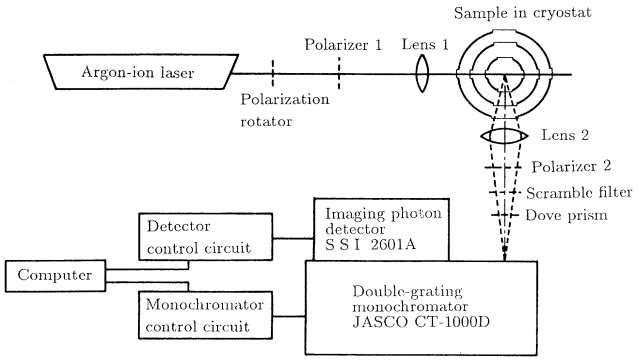

FIG. 1. Block diagram of the experimental system for light scattering from solid helium. For details, see text.

focused into cell with the lens 1, the focal length of which was 100 mm. The light scattered at right angles was gathered with the lens 2 of f/3.7. To analyze the polarization property of the scattered light, the polarizer 2 and the scramble filter were used. The dove prism adjusted the direction of the laser beam image to be parallel to the direction of the inlet slit of the spectrometer. The double grating spectrometer was a JASCO CT1000D. The imaging photon detector (a Surface Sciences Instruments model 2601A) was used for simultaneous detection of whole the spectrum imaged on the two-dimensional surface of outlet slit position of the spectrometer. In order to calibrate weak nonlinearity in the energy shift versus position relation, the rotational Raman spectral peaks of N_2 and O_2 molecules in air were observed. The absolute precision of energy shifts was ± 0.06 cm^{-1}. The observed signals were transferred to the computer for analysis.

The Cu-Be sample cell was cooled with a recirculation-type ^{3}He cryostat. The cell was mounted on the bottom of a pumped liquid ^{3}He bath. The top of the cell could be heated to grow, anneal, or melt helium crystals. Temperature was monitored with a calibrated Ge resister within an accuracy of ± 15 mK. Helium entered the cell through a small capillary tube after being filtered by traps at liquid N_2 temperature and at liquid ^{4}He temperature to eliminate dust or ice particles. We crystallized from superfluid phase to hcp solid phase by increasing the pressure slowly at a constant temperature. In the superfluid phase, residual dust and ice particles were quickly eliminated to negligible level, which could be monitored by a decrease of Tyndall scattering.

III. RESULTS AND DISCUSSION

The lowest temperature we could realize with our ^{3}He cryostat was 0.71 ± 0.05 K under illumination of the incident laser power of 400 mW. The error indicates stability during a measurement run and reproducibility for different runs. In the cooling process of a run, the superfluid sample at a pressure of about 20 kg/cm^2 was cooled down to this temperature. We waited for a while until everything became stable. Tyndall scattering, if any, was also checked and we waited until it became negligible. We then increased the pressure to the value just exceeding the coexistence pressure 24.99 atm (Ref. 16) at 0.71 K. The excess pressure was slightly adjusted manually so that crystallization proceeded slowly enough to obtain a single crystal. The molar volume of hcp solid ^{4}He on the coexisting curve at 0.71 K is 20.98 cm^3/mol.[16] After the crystallization was completed, we increased the pressure up to 30 kg/cm^2 to avoid accidental melting during a run. However, we regard that the molar volume of the sample was kept at the value at the melting curve because the solid phase in the filling capillary prevented further pressurization of the sample.

The experimental spectrum, obtained by adding all our data, is shown in Fig. 2(a). The vertical axis is scaled by counts/sec. Actual total count at the strongest peak P_1 was 118 494 counts. Spectral shape is consistent with those observed in the former work by Slusher and Surko.[13–15] They observed the strong sharp one-phonon peak, which is observed as P_1 here. The energy shift of the peak was 7.39 ± 0.06 cm^{-1} in this experiment. They measured the energy shift ν of the peak as a function of molar volume V_M between 16.5–20.5 cm^3/mol to get a Grüneisen constant of[14]

$$\gamma = -d \ln(\nu)/d \ln(V_M) = 2.6 \pm 0.1 \ .$$

The Grüneisen constant shows a weak molar volume dependence and was obtained as $\gamma = 1.02 + 0.083 V_M$.[14] Extrapolation to a molar volume of 20.98 cm^3/mol yields an energy shift 7.42 cm^{-1}, which is consistent with the value 7.39 ± 0.06 cm^{-1} we observed. A neutron inelastic experiment observed the optical-phonon energy at zero wave vector at 7.50 ± 0.2 cm^{-1} for a molar volume of 21.1 cm^3/mol at 1.03 ± 0.09 K.[5] The neutron result is con-

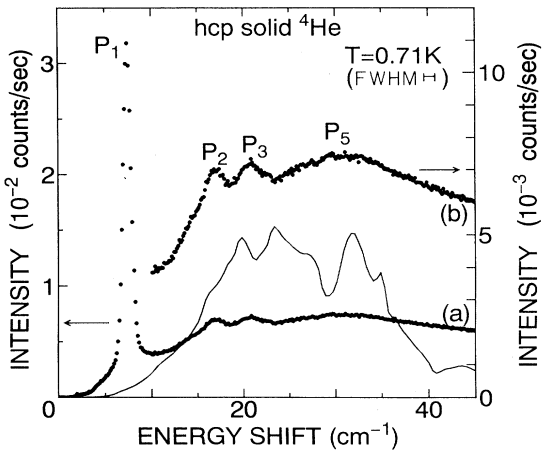

FIG. 2. Raman spectrum of hcp solid ^{4}He obtained by adding all the data measured at a temperature of 0.71 K with an instrumental resolution of 1.1 cm^{-1} (the full width at half maximum). (b) is the same as (a) but expanded by a factor of 3. The peak P_1 corresponds to one-phonon Raman scattering. The peaks P_2, P_3, and P_5 are due to two-phonon Raman scattering. The solid curve is a theoretical two-phonon spectrum for a polycrystalline sample, where the convolution integral was performed to take into account the instrumental resolution profile.

sistent with the Raman results obtained here and by Slusher and Surko.[14]

In the energy region larger than the one-phonon peak, they also observed the two-phonon Raman spectrum as a broad feature peaked at about 45cm^{-1}. What is new in this experiment is that we may claim three peaks P_2, P_3, and P_5 in our observation shown in Fig. 2(a). Those peaks are more clearly seen in Fig. 2(b), where vertical scale is expanded by three times compared with (a) in the energy region from 10 to 45 cm^{-1}. The reason that those were resolved may be due to that sample temperature and instrumental resolution in our work were improved compared with the former work.[13,15] Our values were respectively 0.71 K and 1.1 cm^{-1}, while theirs were 1.4 K and about 4 cm^{-1}. The energy shifts of each peaks P_2, P_3, and P_5 are 17.1 cm^{-1}, 20.9 cm^{-1}, and about 30 cm^{-1}, respectively. More detailed discussion of the structure is given below.

In the large energy shift region where no two-phonon Raman scattering is expected, they observed a substantial continuous spectrum which has a monotonously decreasing dependence on energy shift.[13-15] This feature of the spectra, which is absent in classical solids, was found to correspond to a Raman process of producing a pair of energetic nearly free particles with equal and opposite wave vector. We also observed essentially the same signals, which are not discussed here.

Six normal modes of lattice vibrations are expected from the group theory for a hexagonal close-packed crystal at the zone center. Those are shown in Fig. 3. E_u and E_g include two modes, where atomic displacements are along two different directions in the plane perpendicular to the hexagonal c axis. E_u and A_{2u} are acoustic modes. They could be observed as first-order Brillouin scattering peaks, shifted from the incident laser energy by amounts proportional to their sound velocities multiplied by the magnitude of scattering vector. Due to insufficient instrumental resolution, they are observed as a single central peak S_c of zero energy shift in this experiment. The polarization property of the central component is

$$S_c = S_c^0(\epsilon_f \cdot \epsilon_i)^2 . \tag{1}$$

Here, ϵ_f and ϵ_i are the polarization unit vectors of scattered light and incident light, respectively. Experimentally, ϵ_f is selected by the polarizer 2 in Fig. 1 and ϵ_i by the polarizer 1. The central peak was used as the reference of the energy shift and check of polarizer function.

The one-phonon Raman-active optical mode at the zone center is the E_g mode in Fig. 3, which is observed as P_1 in Fig. 2. According to the theory of Werthamer, Gray, and Koehler (WGK),[12] the polarization property of the one-phonon scattering is

$$S_1(\omega) = S_1^0(\omega)\epsilon_{f\perp}^2 \cdot \epsilon_{i\perp}^2 . \tag{2}$$

Hereafter ($\perp$, $\parallel$) denote (perpendicular, parallel) to the hexagonal c axis.

Various two-phonon processes are possible. The experimental peaks P_2, P_3, and P_5 are detecting a part of these processes. Theoretical numerical calculations were carried out by WGK. Polarization dependence of the two-phonon Raman scattering derived by them is

$$S_2(\omega) = S_{33}(\omega)(\epsilon_{f\parallel} \cdot \epsilon_{i\parallel} - \tfrac{1}{2}\epsilon_{f\perp} \cdot \epsilon_{i\perp})^2 + S_{44}(\omega)\epsilon_{f\perp}^2 \cdot \epsilon_{i\perp}^2 + S_{66}(\omega)|\epsilon_{f\perp} \times \epsilon_{i\parallel} - \epsilon_{f\parallel} \times \epsilon_{i\perp}|^2 . \tag{3}$$

Here, the subscripts are the Voight notation. There are three independent components S_{33}, S_{44}, and S_{66} for the two-phonon Raman scatterings. The results of theoretical calculation for S_{33}, S_{44}, and S_{66} by WGK are also plotted in Fig. 4, by dotted, broken, and dotted-broken curves, respectively. To draw these figures, we reduced the horizontal scale so that the theoretical one-phonon peak position agrees with the experiment. The one-phonon peak is not shown in Fig. 4 for theoretical curves. Because detailed spectral forms of these components are given by WGK and exhibit many fine structures, observation of each spectrum will be fruitful for studies of lattice dynamics. For this purpose, polarization analyses are crucial.

WGK gave procedures to estimate the three components separately. The expression of the one-phonon scattering Eq. (2) implies that a determination of the one-phonon scattering intensity as a function of polarization suffices to fix uniquely the c axis relative to the scattering axes, which in turn allows an unambiguous computation of the three scalar combinations appearing in Eq. (3) once ϵ_f and ϵ_i are given. Thus the one-phonon scattering is itself sufficient in determining the crystal

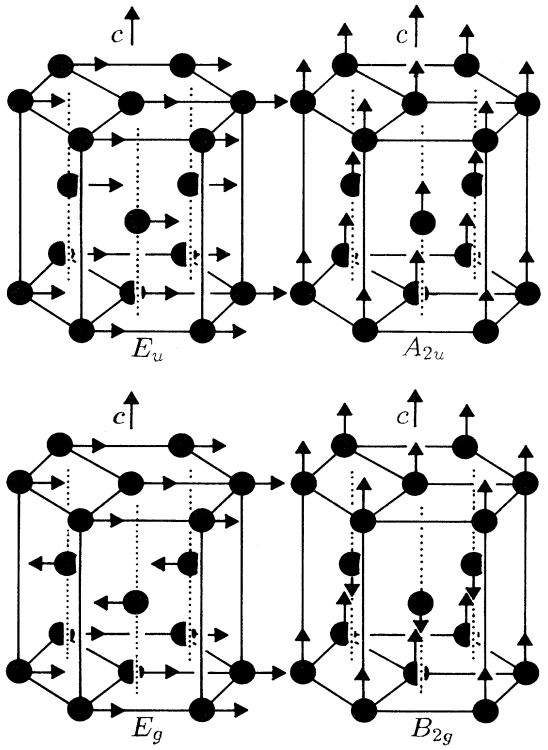

FIG. 3. The normal modes of lattice vibrations in the hcp ^{4}He at the zone center in the wave-vector space.

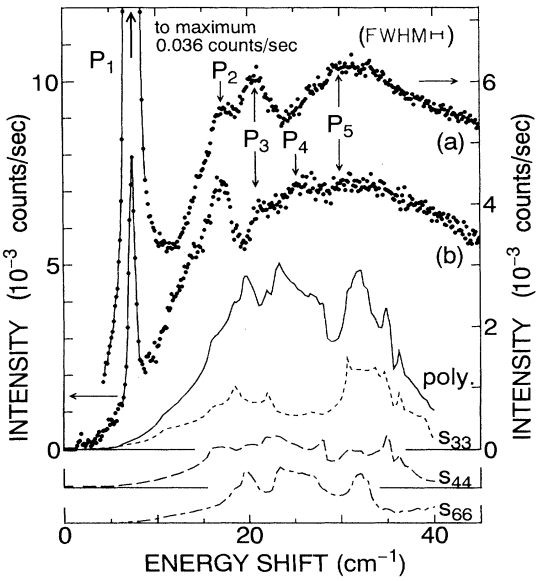

FIG. 4. Raman spectra of hcp solid ^{4}He at 0.71 K obtained by adding artificially selected data. (a) is the addition of a set of data, where the one-phonon peak P_1 is more than seven times stronger than the two-phonon scattering P_2-P_5. (b) is the addition of a set of data, where the one-phonon peak is comparable or weaker than the two-phonon peaks. We can observe clear differences in the relative intensities of the two-phonon peaks. S_{33}, S_{44}, and S_{66} are theoretical spectra expected for different conditions of polarization. The solid line is the theoretical spectrum expected for a polycrystalline sample.

orientation to obtain all the three tensor components of the two-phonon scattering.

We carried out polarization analysis of the one-phonon peak P_1. In fact, rotation of either ϵ_i or ϵ_f results in a clear change of the peak intensity. The above-mentioned first step to determine the c-axis direction was possible. However, a single run of our cryostat was limited within about three days due to the liquid-helium supply policy of our institute. A measuring time of about 60 h for a single run was not sufficient enough to observe the two-phonon Raman structure with a good statistical accuracy. Although we could prepare a single crystal for each run, crystal orientation in the cell could not be controlled. In different runs, we could not reproduce the same polarization condition for the two-phonon processes. Therefore, we could not proceed further in the procedure of WGK for precise separate estimations of the three components S_{33}, S_{44}, and S_{66}.

However, we could carry out imperfect but still informative polarization analysis by classifying our data. To select one set of data out of all our results, we picked up spectra in which the peak intensity of the one-phonon peak P_1 is comparable or less compared with the intensity of two-phonon Raman scattering. The resultant summation of the spectra is shown in Fig. 4(b). For this, Eq. (2) indicates both $\epsilon_{f\perp}$ and $\epsilon_{i\perp}$ to be small. Then contributions of S_{44} and perhaps also S_{66} to the spectrum are expected to be small from Eq. (3). Therefore the spectrum may reflect feature characteristics for S_{33}.

To get another set of data, we gathered spectra in which the peak intensity of P_1 is more than seven times stronger than the intensity of the two-phonon spectrum. The resultant sum is shown in Fig. 4(a). In this case, the contribution of S_{44} is expected to be larger from Eqs. (2) and (3) compared with the spectrum (b).

We can observe clear differences between (a) and (b). The peak P_4 is observed for (b), which is not clear for (a). Relative intensities of the peaks are different for the two spectra. The clear sensitive dependence of the spectrum on crystal orientation and polarization directions supports the proposal by WGK that the parameters of lattice dynamics may be obtained from the structures of the two-phonon Raman scattering. To make a quantitative analysis, however, present results lack definitive information of crystal orientation, instrumental resolution to resolve sharp peaks, and vertical accuracy to confirm weak peaks.

The polycrystalline two-phonon spectrum was related to the three components of the two-phonon Raman scattering by WGK as

$$S_2(\omega)_{\text{poly}}=\tfrac{3}{5}[\tfrac{1}{4}S_{33}(\omega)+\tfrac{2}{3}S_{44}(\omega)+\tfrac{2}{3}S_{66}(\omega)] \times[1+\tfrac{1}{3}(\epsilon_f\cdot\epsilon_i)^2]\ . \quad (4)$$

The theoretical spectrum is shown in Fig. 4 by the solid curve. To compare the theoretical spectrum with experiment, it should be convoluted with the instrumental resolution function. The result of the convolution of the theoretical spectrum with a Gaussian function of 1.1 cm^{-1} full width at half maximum is plotted in Fig. 2 by the solid curve.

The experimental spectrum shown in Fig. 2, obtained by adding all the spectra, is expected to be similar to the theoretical polycrystalline spectrum. The former is the sum of spectra for crystals of various orientations with respect to experimental optical axis. But it would not be exactly the same because there might have been some preferential orientation of crystal growth. Anyway, the overall features of the experimental and theoretical spectra show good qualitative similarity. The three main peaks in the theoretical spectrum can be related to the peaks P_2, P_3, and P_5. Those theoretical peaks are superpositions of unresolved sharp peaks, as expected from the separate plots of S_{33}, S_{44}, and S_{66}. Therefore further detailed analyses of the peak positions cannot be carried out clearly. However, the similarity verify that the theoretical spectra calculated by WGK successfully postulated what are expected for the two-phonon Raman scattering of the hcp solid ^{4}He. They also calculated the Raman spectrum of bcc solid ^{3}He. Once fully accurate experimental spectra of quantum solids have been obtained for various polarization conditions with sufficient resolution in the future, adjusting the parameters in the WGK model to fit theoretical spectra to experiment will be able to yield quantities relevant to lattice dynamics of quantum solids.

Finally, conditions necessary for future experimental works to make a full comparison with the WGK theory is suggested. The theoretical spectra exhibit subtle weak

and sharp features, which should be observed by an experiment to make a quantitative analysis to determine the parameters of lattice dynamics. To resolve them, we need an experimental resolution of better than about 0.2 cm^{-1}, which is about five times better than that realized in this experiment. Intensity will be decreased roughly proportional to the instrumental width of resolution. Statistical accuracy of data points must exceed about $\pm 0.5\%$ to observe a variation comparable with weak features in the theory, while present accuracy is about 3% at best. To improve the statistical accuracy by a factor of 10, a hundred times longer measuring time is necessary.

ACKNOWLEDGMENTS

We would like to thank Professor K. Nagai for valuable discussions. Thanks are also due H. Sasaki for his collaboration during measurements. This work is supported by a Grant-in-Aid for Scientific Research from the Ministry of Education, Science, and Culture of Japan.

[1]K. Ohbayashi and M. Udagawa, Phys. Rev. B **31**, 1324 (1985).
[2]K. Ohbayashi, in *Elementary Excitations in Quantum Fluids,* edited by K. Ohbayashi and M. Watabe (Springer-Verlag, Berlin, 1989), p. 32.
[3]K. Ohbayashi, in *Excitation in Two-Dimensional and Three-Dimensional Quantum Fluids,* edited by A. F. G. Wyatt and H. J. Lauter (Plenum, New York, 1991), p. 77.
[4]F. P. Lipschultz, V. J. Minkiewicz, T. A. Kitchens, G. Shirane, and R. Nathans, Phys. Rev. Lett. **19**, 1307 (1967).
[5]V. J. Minkiewicz, T. A. Kitchens, F. P. Lipschultz, R. Nathans, and G. Shirane, Phys. Rev. **174**, 267 (1968).
[6]T. R. Koehler, Phys. Rev. Lett. **18**, 654 (1967).
[7]T. R. Koehler, Phys. Rev. **165**, 942 (1968).
[8]N. S. Gillis, T. R. Koehler, and N. R. Werthamer, Phys. Rev. **175**, 1110 (1968).
[9]N. S. Gillis and N. R. Werthamer, Phys. Rev. **167**, 607 (1968).
[10]T. J. Greytak and J. Yan, Phys. Rev. Lett. **22**, 987 (1969).
[11]N. R. Werthamer, Phys. Rev. **185**, 348 (1969).
[12]N. R. Werthamer, R. L. Gray, and T. R. Koehler, Phys. Rev. B **4**, 1324 (1971).
[13]R. E. Slusher and C. M. Surko, Phys. Rev. Lett. **27**, 1699 (1971).
[14]R. E. Slusher and C. M. Surko, Phys. Rev. B **13**, 1086 (1976).
[15]C. M. Surko and R. E. Slusher, Phys. Rev. B **13**, 1095 (1976).
[16]E. R. Grilly, J. Low Temp. Phys. **11**, 33 (1973).